The target then shifted randomly to left or right horizontal peripheral locations (10 degrees from the center position), where it remained for 1000 ms. The target size was 1 degree of the visual angle. The number of left and right saccadic eye movements was the same. Participants were instructed to follow the target as quickly and accurately as possible, alternating between 40 s of control condition task and 40 s of prosaccade condition, completing 10 sets of trials in all. During the baseline condition, subjects were in total darkness and were asked to maintain fixation and not blink.

Antisaccade task

The parameters for the antisaccade task were identical to those for the prosaccade task. The antisaccade task required participants to fixate the target in the central position and to redirect their gaze in the opposite direction of the target as soon as it shifted to the periphery. Participants performed 10 sets of trials in total, alternating antisaccade and control conditions.

fMRI data analysis

Image analysis was performed using an Ultra5 workstation (Sun Microsystems, Palo Alto, CA, USA) using MATLAB (Mathworks Inc., Natick, MA, USA) and statistical mapping (SPM99, Wellcome Department of Cognitive Neurology, London, UK; http://www.fil.ion.ucl.ac.uk/spm). Before statistical parametric maps were calculated, EPI images for each time series were realigned to the first functional image to remove residual head movement. Images were then coregistered and normalized to the Montreal National Institute template. Confounding effects of global volume activity and magnetic noise were removed using linear regression and cosine functions (up to a maximum of 1 cycle per 40 scans). Removing the latter confounds corresponds to high-pass filtering of the time series to remove low-frequency artifacts that can arise due to aliased cardiac and other cyclical components. After normalization, three-dimensional spatial smoothing was applied to each volume using a Gaussian kernel of $8 \times 8 \times 8$ mm. Alternating periods of baseline and activation were modeled using a simple delayed box-car reference vector to account for delayed cerebral blood flow after stimulus presentation. Significantly activated pixels were searched for using the General Linear Model approach for time-series data.

To create the subtraction activation image between saccade and antisaccade, data was analyzed using random-effect analysis. Statistical significance was set at the level of $P < 0.001$, uncorrected for multiple comparisons.

Intra-individual comparisons between saccade and antisaccade were analyzed using paired *t*-tests, and statistical significance was set at the level of $P < 0.005$, uncorrected for multiple comparisons.

RESULTS

Behavioral data

Demographic and performance data are summarized in Table 1. The analysis of EOG revealed no differences in prosaccades between the patients and normal controls. In contrast, error rates in antisaccades were higher and latencies of prosaccades and antisaccades were longer in the patient group than in the control group.

fMRI data

Activated areas in the normal control group are shown in Fig. 1a for the saccade tasks and in Fig. 1b for the antisaccade tasks ($P < 0.001$, uncorrected for multiple comparisons). During the saccade tasks, regional activations were observed bilaterally in the frontal eye fields (FEF), supplementary eye fields (SEF), and parietal eye fields (PEF), left lenticular

Table 1. Subjects and eye movement performance

	Patients with Schizophrenia	Control
Number of cases (male/female)	18 (12/6)	18 (9/9)
Age (year)	34.8 ± 7.9	37.6 ± 4.8
Education (year)*	11.2 ± 2.9	15.3 ± 2.2
Age at the onset (year)	25.8 ± 6.4	–
HPD equivalence (mg)	16.0 ± 16.1	–
BPRS total score	41.9 ± 7.9	–
Saccade error (%)*	0.5 ± 0.67	0.00 ± 0.00
Saccade latency (ms)*	212.2 ± 30.1	174.2 ± 11.8
Anti-saccade error (%)*	1.1 ± 1.6	0.14 ± 0.35
Anti-saccade latency (ms)*	244.9 ± 48.4	205.6 ± 18.5

Statistical analysis (T-test) *$P < 0.05$.
BPRS, Brief Psychiatric Rating Scale; HPD, haloperidol.

© 2009 The Authors
Journal compilation © 2009 Japanese Society of Psychiatry and Neurology

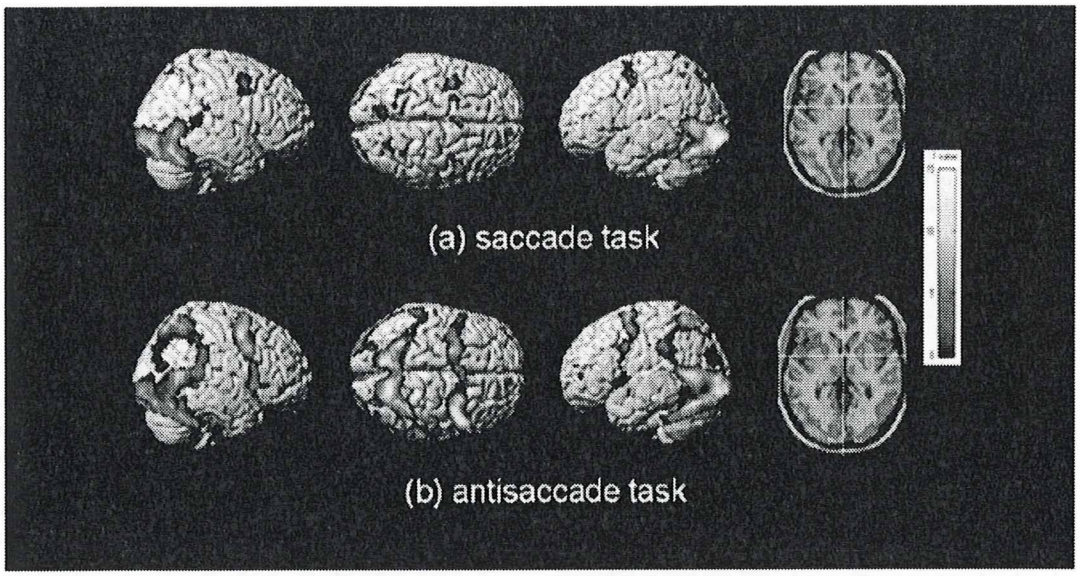

Figure 1. Brain regions displaying greater activities during (a) saccade and (b) antisaccade conditions than during control condition in healthy subjects. In the rightmost image, the activation map is overlaid onto a T1 SPM normalized brain image. The height threshold is set at $P < 0.001$, uncorrected.

nucleus, and bilateral occipital cortices (V1). During the antisaccade tasks, activations were observed in the same regions as during saccade tasks, as well as bilaterally in the inferior parietal lobules (IPL), thalami, right lenticular nucleus, inferior frontal gyrus (IFG), and left dorsolateral prefrontal cortex (DLPFC) (Table 2).

Activation areas in the patient group are shown in Fig. 2a for the saccade tasks and in Fig. 2b for the antisaccade tasks ($P < 0.001$, uncorrected for multiple comparisons). During the saccade task, regional activation was observed bilaterally in the FEF, SEF, and PEF, left lenticular nucleus, and V1. These regions are the same as those seen in the normal subject group. However, the patient group also showed activations in the IFG, DLPFC, IPL, lenticular nucleus and thalamus during saccade tasks. During the antisaccade tasks, activation was observed in the same regions as in the saccade tasks (Table 3).

Furthermore, in the normal control group, comparing brain activity during the antisaccade task with that during the saccade task revealed that antisaccade eye movements induced elevated activities in the bilateral FEF, PEF, IPL, ACC, IFG, and DLPFC ($P < 0.005$, uncorrected for multiple comparisons). In the patient group, however, only bilateral activation in the PEF was observed.

Correlation between fMRI activation and eye movement performance

In order to assess the effect of performance on brain activity, we analyzed the correlation between error rate and brain activity. Figure 3 shows the correlation between fMRI activation and eye movement performance in patients with schizophrenia. fMRI activation is calculated from each peak voxel. No significant correlation was observed between two parameters.

DISCUSSION

Our understanding of human cortical control of saccades is derived from observations of cerebral lesions[14–18] and from transcranial magnetic stimulation,[37,38] positron emission tomography,[19,20] and fMRI.[21–24] Previous studies in these areas have indicated that saccadic eye movements are controlled by

© 2009 The Authors
Journal compilation © 2009 Japanese Society of Psychiatry and Neurology

Table 2. Brain regions more active during visually guided saccades and antisaccades than during control tasks in healthy subject

Brain region		Saccade vs rest Coordinate			t-value	Antisaccade vs rest Coordinate			t-value
		X	*Y*	*Z*		*X*	*Y*	*Z*	
DLPFC	R	–	–	–	NS	*50*	*40*	*–8*	4.01
	L	–	–	–	NS	*–44*	*50*	*4*	4.24
FEF	R	*46*	*6*	*50*	5.34	*40*	*–2*	*50*	5.87
	L	*–40*	*–6*	*50*	6.08	*–38*	*–4*	*52*	6.52
SEF	R	*6*	*6*	*62*	4.20	*8*	*8*	*52*	4.20
	L	*–4*	*4*	*60*	5.87	*–2*	*10*	*46*	5.56
PEF	R	*32*	*–54*	*48*	3.80	*26*	*–58*	*54*	6.70
	L	*–30*	*–56*	*56*	4.28	*–26*	*–60*	*52*	7.91
IPL	R	–	–	–	NS	*64*	*–36*	*28*	6.14
	L	–	–	–	NS	*–64*	*–40*	*34*	5.75
Thalamus	R	*–12*	*–18*	*10*	3.96	*10*	*–14*	*8*	8.30
	L	*–10*	*–18*	*–2*	6.53	*–10*	*–16*	*8*	6.29

DLPFC, dorsolateral prefrontal cortex; FEF, frontal eye fields; IPL, inferior parietal lobule; L, left; NS, not significant; PEF, parietal eye fields; R, right; SEF, supplementary eye fields.

a cortical network that includes the PEF, located in the intraparietal sulcus and superior parietal lobule, the FEF, located in the precentral gyrus, and the SEF, located in the upper medial wall of the frontal lobe. Activation has also been observed in the bilateral dorsolateral prefrontal cortices, supramarginal gyri, anterior cingulate cortices, and thalami during antisaccade tasks.[35] In short, in normal subjects no

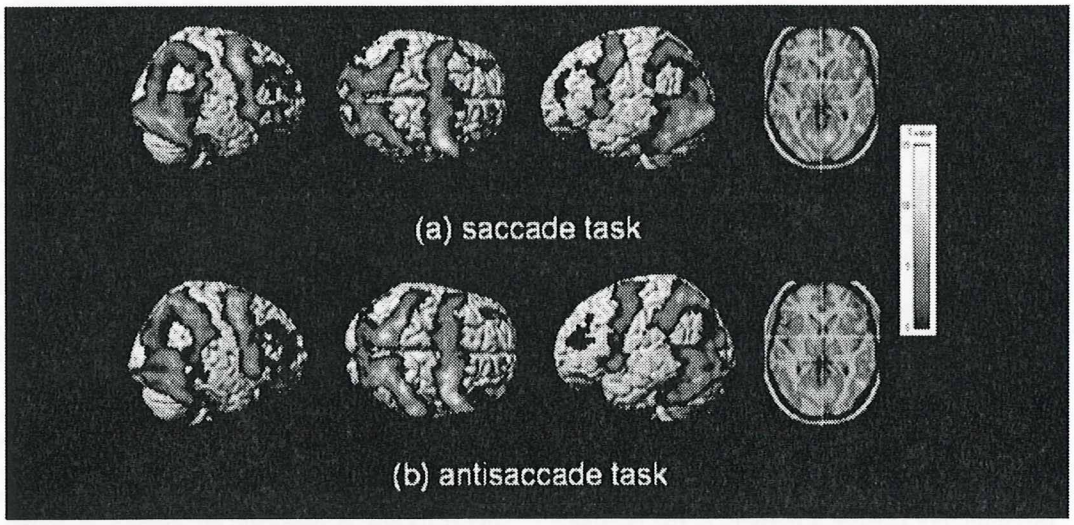

Figure 2. Brain regions displaying greater activities during (a) saccade and (b) antisaccade conditions than during control conditions in patients with schizophrenia. In the rightmost image, the activation map is overlaid onto a T1 SPM normalized brain image. The height threshold is set at $P < 0.001$, uncorrected.

© 2009 The Authors
Journal compilation © 2009 Japanese Society of Psychiatry and Neurology

Table 3. Brain regions more active during visually guided saccades and antisaccades than during control tasks in patients with schizophrenia

		Saccade vs rest Coordinate				Antisaccade vs rest Coordinate			
Brain region		*X*	*Y*	*Z*	*t*-value	*X*	*Y*	*Z*	*t*-value
DLPFC	R	36	56	26	8.80	42	56	8	6.05
	L	−38	54	14	4.26	−36	44	12	5.00
FEF	R	34	2	64	8.52	26	0	48	12.06
	L	−44	−4	58	9.91	−36	−6	46	8.99
SEF	R	12	16	38	5.38	10	4	48	5.30
	L	−8	22	38	5.23	−12	0	46	5.53
PEF	R	30	−54	48	7.25	22	−60	54	12.32
	L	−28	−52	50	10.71	−28	−52	56	12.89
IPL	R	56	−32	22	8.63	62	−38	18	5.09
	L	−58	−40	22	3.77	−62	−38	18	4.27
Thalamus	R	12	−14	2	6.70	10	−18	−4	7.09
	L	−12	−14	−2	6.92	−12	−16	2	6.23

DLPFC, dorsolateral prefrontal cortex; FEF, frontal eye fields; IPL, inferior parietal lobule; L, left; PEF, parietal eye fields; R, right; SEF, supplementary eye fields.

activation of DLPFC, IFG, striatum, and thalamus were observed during the saccade tasks.

Contrary to previous reports, the present study showed the activations in the DLPFC, IFG, striatum, and thalamus during both the saccade and antisaccade tasks in patients with schizophrenia. In addition, differential activation maps between the antissacade and saccade tasks exhibited the bilateral activation of the FEF, PEF, IPL, ACC, IFG, and DLPFC in normal subjects, whereas only the PEF were activated bilaterally in the patient group. These results show that normal subjects process the saccade and antisaccade tasks in different brain regions, whereas patients with schizophrenia likely use virtually the same regions when processing both tasks. In the patient group, therefore, when brain activations during eye movement tasks were compared directly, the elevated activations of the DLPFC and thalamus normally seen in antisaccade tasks relative to saccade tasks were no longer observed. In comparing the patients to the normal controls, the present study demonstrated higher activity of the thalamus and broad cortical regions (including the prefrontal area), especially during saccade tasks. This suggests hyperactivation, not reduced activation, in the prefrontal cortex and thalamus in patients with schizophrenia. Taken together, though the antisaccade task is cognitively more demanding than the saccade task, these regions in the patients with schizophrenia did not seem to be activated at a level that corresponded to the degree of difficulty of the tasks presented.

The tasks used in most of the previous studies required subjects to focus on a gazing point, and the reduced activities of the DLPFC and thalamus were observed during the antisaccade tasks in patients with schizophrenia. Three recent studies using fMRI revealed reduced activation in the right DLPFC and reduced activation in the striatum in schizophrenia.[16–17]

In contrast, our results showed higher activities in broad cortical and subcortical regions during the saccade and antisaccade tasks in the patient group as compared with the normal control group. This suggests that these regions could already be activated by the time the schizophrenic patient focuses on the gazing point; therefore, the difference in activation levels between baseline and eye movements becomes smaller in the patient group.

In the present study, we demonstrated the activations in the DLPFC and thalamus during the saccade task in the patient group. The fronto-striato-thalamo-cortical network,[26–28] including the prefrontal cortex and thalamus, is important for control of antisaccades. Schizophrenia presents with dysfunction in dopaminergic neural networks[29] and the fronto-striato-thalamic circuit.[30,31] Dysfunction in the

© 2009 The Authors
Journal compilation © 2009 Japanese Society of Psychiatry and Neurology

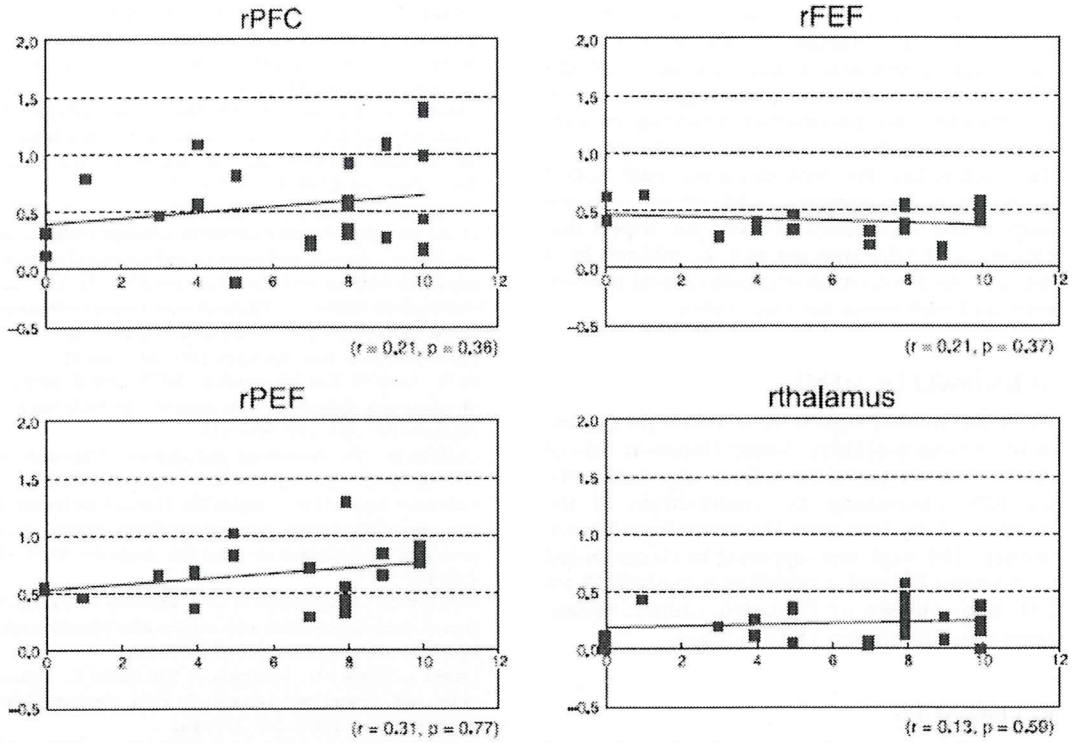

Figure 3. The correlation between brain activation and the number of antisaccade errors. The horizontal axis represents the number of antisaccade errors, and the vertical axis represents the estimated magnetic resonance imaging signal. rFEF, right frontal eye fields; rPEF, right parietal eye fields; rPFC, right prefrontal cortex; rthalamus, right thalamus.

striato-thalamo-cortical dopaminergic circuitry may reduce inhibition of reflexive saccade and thus facilitate saccades for the target direction during the antisaccade task in schizophrenics. Our results indicate that this dysfunction has an important influence on subtle motor control and therefore affects antisaccade generation through both the direct and indirect basal ganglia pathways. These findings suggest that patients with schizophrenia who display antisaccade inhibition errors may present with dysfunction in the fronto-striato-thalamo-cortical network.

Given that previous studies have targeted patients with schizophrenia with poor performance in cognitive tasks, a bias toward reduced brain activations may have been present.[32–36] In order to assess the effect of performance on brain activity, we analyzed the correlation between error rate and brain activity. No significant correlation was observed between the two variables. Therefore, we conclude that the performance did not directly affect the results.

CONCLUSION

In order to examine baseline effect, we employed an eye movement task that did not require subjects to focus on a fixation point during the baseline condition, and compared brain activity between patients with schizophrenia and normal control subjects. In normal subjects, activities in the DLPFC and thalamus were greater during antisaccade tasks than during saccade tasks, whereas no significant difference was observed in patients with schizophrenia. These results suggest that the brains of patients with schizophrenia did not seem to be activated at a level that corresponded to the degree of difficulty of the tasks presented. Previous studies that used target fixa-

© 2009 The Authors
Journal compilation © 2009 Japanese Society of Psychiatry and Neurology

tion at baseline assessment showed reduced activities of the DLPFC and thalamus in patients. In contrast, our study demonstrated hyperactivation of the DLPFC and thalamus in patients, suggesting that in patients with schizophrenia these brain regions were already activated by the time patients viewed a fixed target at baseline. We think that these results reflect the symptom that patients of schizophrenia can not adapt to the environment. Finally, we suspect that patients with schizophrenia may be affected by a defect in the fronto-striato-thalamo-cortical network associated with motor function control.

ACKNOWLEDGMENT

We thank Professor Makoto Uchiyama of the Department of Neuropsychiatry, Nihon University School of Medicine for providing helpful suggestions. We gratefully acknowledge the contributions of the members of the Tamagawa University Brain Science Institute. This work was supported by Grants-in-Aid for Scientific Research #19790838 & #18300275 for T.M. from Ministry of Education, Culture, Sports, Science and Technology (MEXT), Japan.

REFERENCES

[3] Iacono WG, Tuason VB, Johnson RA. Dissociation of smooth-pursuit and saccadic eye tracking in remitted schizophrenics. An ocular reaction time task that schizophrenic perform well. *Arch. Gen. Psychiatry* 1981; 38: 991–996.

[7] Levin S, Holzman PS, Rothenberg SJ, Lipton RB. Saccadic eye movements in psychotic patients. *Psychiatry Res.* 1981; 5: 47–58.

[5] Levin S, Jones A, Stark L, Merrin EL, Holzman PS. Identification of abnormal patterns in eye movements of schizophrenic patients. *Arch. Gen. Psychiatry* 1982; 39: 1125–1130.

[4] Fukushima J, Fukushima K, Chiba T, Tanaka S, Yamashita I, Kato M. Disturbances of voluntary control of saccadic eye movements in schizophrenic patients. *Biol. Psychiatry* 1988; 23: 670–677.

[6] Everling S, Fischer B. The antisaccade: A review of basic research and clinical studies. *Neuropsychologia* 1998; 36: 885–899.

[8] Sereno AB, Holzman PS. Antisaccades and smooth pursuit eye movements in schizophrenia. *Biol. Psychiatry* 1995; 37: 394–401.

[7] McDowell JE, Clementz BA. The effect of fixation condition manipulations on antisaccade performance in schizophrenia: Studies of diagnostic specificity. *Exp. Brain. Res.* 1997; 115: 333–344.

[8] Fukushima J, Morita N, Fukushima K, Chiba T, Tanaka S, Yamashita I. Voluntary control of saccadic eye movements in patients with schizophrenic and affective disorders. *J. Psychiatr. Res.* 1990; 24: 9–24.

[9] Crawford TJ, Sharma T, Puri BK, Murray RM, Berridge DM, Lewis SW. Saccadic eye movements in families multiply affected with schizophrenia: The Maudsley Family Study. *Am. J. Psychiatry* 1998; 155: 1703–1710.

[10] Raemaekers M, Jansma JM, Cahn W *et al.* Neuronal substrate of the saccadic inhibition deficit in schizophrenia investigated with 3-dimensional event-related functional magnetic resonance imaging. *Arch. Gen. Psychiatry* 2002; 59: 313–320.

[11] McDowell JE, Brown GG, Paulus M *et al.* Neural correlates of refixation saccades and antisaccades in normal and schizophrenia subjects. *Biol. Psychiatry* 2002; 51: 216–223.

[12] Tu PC, Yang TH, Kuo WJ, Hsieh JC, Su TP. Neural correlates of antisaccade deficits in schizophrenia, an fMRI study. *J. Psychiatry Res.* 2006; 40: 606–612.

[13] Oldfield RC. The assessment and analysis of handedness: The Edinburgh inventory. *Neuropsychologia* 1971; 9: 97–113.

[14] Guitton D, Buchtel HA, Douglas RM. Frontal lobe lesions in man cause difficulties in suppressing reflexive glances and in generating goal-directed saccades. *Exp. Brain Res.* 1985; 58: 455–472.

[15] Evdokimidis I, Liakopoulos D, Constantinidis TS, Papageorgiou C. Cortical potentials with antisaccades. *Electroencephalogr. Clin. Neurophysiol.* 1996; 98: 377–384.

[16] Crevits L, Hanse MC, Tummers P, Van Maele G. Antisaccades and remembered saccades in mild traumatic brain injury. *J. Neurol.* 2000; 247: 179–182.

[17] Kapoula Z, Isotalo E, Muri RM, Bucci MP, Rivaud-Péchoux S. Effects of transcranial magnetic stimulation of the posterior parietal cortex on saccades and vergence. *Neuroreport* 2001; 12: 4041–4046.

[18] Leff AP, Scott SK, Rothwell JC, Wise RJ. The planning and guiding of reading saccades: A repetitive transcranial magnetic stimulation study. *Cereb. Cortex.* 2001; 11: 918–923.

[19] Anderson TJ, Jenkins IH, Brooks DJ, Hawken MB, Frackowiak RS, Kennard C. Cortical control of saccades and fixation in man. A PET study. *Brain* 1994; 117: 1073–1084.

[20] O'Driscoll GA, Wolff AL, Benkelfat C, Florencio PS, Lal S, Evans AC. Functional neuroanatomy of smooth pursuit and predictive saccades. *Neuroreport* 2000; 11: 1335–1340.

[21] Gaymard B, Ploner CJ, Rivaud-Péchoux S, Pierrot-Deseilligny C. The frontal eye field is involved in spatial short-term memory but not in reflexive saccade inhibition. *Exp. Brain Res.* 1999; 129: 288–301.

[22] Connolly JD, Goodale MA, Desouza JF, Menon RS, Vilis T. A comparison of frontoparietal fMRI activation during anti-saccades and anti-pointing. *J. Neurophysiol.* 2000; 84: 1645–1655.

[23] Nobre AC, Gitelman DR, Dias EC, Mesulam MM. Covert visual spatial orienting and saccades: Overlapping neural systems. *Neuroimage* 2000; 11: 210–216.

© 2009 The Authors
Journal compilation © 2009 Japanese Society of Psychiatry and Neurology

[24] Matsuo K, Kato C, Sumiyoshi C *et al.* Discrimination of Exner's area and the frontal eye field in humans: Functional magnetic resonance imaging during language and saccade tasks. *Neurosci. Lett.* 2003; 340: 13–16.
[25] Matsuda T, Matsuura M, Ohkubo T *et al.* Functional MRI mapping of brain activation during visually guided saccades and antisaccades: Cortical and subcortical networks. *Psychiatry Res. Neuroimaging.* 2004; 131: 147–155.
[26] Alexander GE, DeLong MR, Strick PL. Parallel organization of functionally segregated circuits linking basal ganglia and cortex. *Annu. Rev. Neurosci.* 1986; 9: 357–381.
[27] Petit L, Orssaud C, Tzourio N, Salamon G, Mazoyer B, Berthoz A. PET study of voluntary saccadic eye movements in humans: Basal ganglia-thalamocortical system and cingulate cortex involvement. *J. Neurophysiol.* 1993; 69: 1009–1017.
[28] McFarland NR, Haber SN. Thalamic relay nuclei of the basal ganglia form both reciprocal and nonreciprocal cortical connections, linking multiple frontal cortical areas. *J. Neurosci.* 2002; 22: 8117–8132.
[29] Gerfen CR, Engber TM, Mahan LC *et al.* D1 and D2 dopamine receptor-regulated gene expression of striatonigral and striatopallidal neurons. *Science* 1990; 250: 1429–1432.
[30] Buchsbaum MS, Haier RJ, Potkin SG *et al.* Frontostriatal disorder of cerebral metabolism in never-medicated schizophrenics. *Arch. Gen. Psychiatry* 1992; 49: 935–942.
[31] Camchong J, Dyckman KA, Chapman CE, Yanasak NE, McDowell JE. Basal ganglia-thalamocortical circuitry disruptions in schizophrenia during delayed response tasks. *Biol. Psychiatry* 2006; 60: 235–241.
[32] Frith CD, Friston KJ, Herold S *et al.* Regional brain activity in chronic schizophrenic patients during the performance of a verbal fluency task. *Br. J. Psychiatry* 1995; 167: 343–349.
[33] Price CJ, Friston KJ. Scanning patients with tasks they can perform. *Hum. Brain Mapp.* 1999; 8: 102–108.
[34] Bullmore E, Brammer M, Williams SC *et al.* Functional MR imaging of confounded hypofrontality. *Hum. Brain Mapp.* 1999; 8: 86–91.
[35] Callicott JH, Bertolino A, Mattay VS *et al.* Physiological dysfunction of the dorsolateral prefrontal cortex in schizophrenia revisited. *Cereb. Cortex.* 2000; 10: 1078–1092.
[36] Jansma JM, Ramsey NF, Coppola R, Kahn RS. Specific versus nonspecific brain activity in a parametric N-back task. *Neuroimage* 2000; 12: 688–697.

© 2009 The Authors
Journal compilation © 2009 Japanese Society of Psychiatry and Neurology

Environmentalist (2009) 29:186–189
DOI 10.1007/s10669-008-9199-8

Direct observation of microcirculatory parameters in rat brain after local exposure to radio-frequency electromagnetic field

S. Hirota · M. Matsuura · H. Masuda · A. Ushiyama · K. Wake · S. Watanabe · M. Taki · C. Ohkubo

Published online: 25 November 2008
© Springer Science+Business Media, LLC 2008

Abstract A cranial window method modified for our experiment enabled to observe the cerebral microcirculation including the blood-brain barrier permeability after a local expose to radio-frequency electromagnetic fields with a monopole antenna in rats. The present report reviews our recent publications that reported no noticeable changes in the cerebral microcirculatory parameters due to RF-EMF exposure.

Keywords Radio-frequency electromagnetic field · Blood-brain barrier · Leukocyte behaviors · Plasma velocity

S. Hirota (✉) · M. Matsuura
Department of Life Science and Bio-informatics, Division of Biomedical Laboratory Sciences, Graduate School of Health Sciences, Tokyo Medical and Dental University, 1-5-45 Yusima, Bunkyo-ku, Tokyo 113-8519, Japan
e-mail: hirota_shi@yahoo.co.jp

H. Masuda
Laboratoire IMS-Site ENSCPB, Bordeaux 1, 16 av., Pey Berland, 33607 Pessac cedex, France

S. Hirota · A. Ushiyama
Department of Environmental Health, National Institute of Public Health, 2-3-6 Minimi, Wako-shi, Saitama 351-0197, Japan

K. Wake · S. Watanabe
Electromagnetic Compatibility Group, Applied Electromagnetic Research Center, National Institute of Information and Communications Technology, 4-2-1 Nukui-kitamachi, Koganei, Tokyo 184-8795, Japan

M. Taki
Department of Electrical and Electronic Engineering, Tokyo Metropolitan University, 1-1 Minami-osawa, Hachioji, Tokyo 192-0397, Japan

C. Ohkubo
Department of Environmental Biology, Meiji Pharmaceutical University, 2-522-1 Noshio, Kiyose, Tokyo 204-8588, Japan

C. Ohkubo
Japan EMF Information Center, 2-9-11 Shiba, Minato-ku, Tokyo 105-0014, Japan

1 Introduction

The possibility of radio-frequency electromagnetic fields (RF-EMF) of mobile phones causing any adverse health effects is still a subject of many studies. One of the most remarkable findings in recent years was the change in permeability of blood-brain barrier (BBB) related to RF-EMF exposure (Salford et al. 1994). Most of these studies, however, have been performed by the histological investigations due to postmortem examination (Salford et al. 1994; Tsurita et al. 2000; Finnie et al. 2006; Fritze et al. 1997). On the other hand, little information is available about the effects of RF-EMF exposure on cerebral microcirculation. A closed cranial window (CCW) method has been widely used among many researchers as a beneficial method to observe the cerebral microcirculation directly. In particular, the changes in BBB function, leukocyte behavior, and plasma velocity were measured as a cerebral microcirculatory parameter (Masuda et al. 2000, 2007a; Mayhan 2001; Yuan et al. 2003). We partially modified this method for evaluating the effects of exposure to RF-EMF on the cerebral microcirculation (Masuda et al. 2000, 2007a). Our recent studies investigated the effect of acute or subchronic exposure to RF-EMF on the cerebral microcirculation in rats using the monopole antenna that enabled local exposure to the brain (Masuda et al. 2007b, c).

2 Materials and methods

Male Sprague–Dawley rats were used in two exposure experiments: acute (10–11 weeks old, 386 ± 22 g, Tokyo Laboratory Animals Science Co. Ltd, Japan) and subchronic (10–11 weeks old, 404 ± 36 g). They were fed a standard pellet diet and water ad libitum and were maintained with a 12 h light/dark cycle, at a temperature of 23.0 ± 1°C and a relative humidity of 50 ± 10%. All experimental procedures were conducted in accordance with the ethical guidelines for animal experiments at the National Institute of Public Health, Japan.

The CCW setup was developed with acryl, plastic, and glass, but no metal materials (Masuda et al. 2007a). The CCW was implanted into the parietal region of the anesthetized rats with intramuscular injection of ketamine (100 mg/kg) and xylazine (10 mg/kg). After removal of hair, skin, and connective tissue from the parietal region, a 10-mm circular hole was made in the parietal skull. Subsequently, the dura mater and arachnoid were carefully removed from the cerebral surface to expose the pia mater. The window was inserted into the hole of the skull and fixed with glue. All animals were used for the experiment at least 1 week after the window implantation to allow for recovery (Fig. 1).

The exposure system we used consisted of a small anechoic chamber and a monopole antenna. The head of each rat was positioned toward the central antenna and was locally exposed to 1,439 MHz electromagnetic near-field

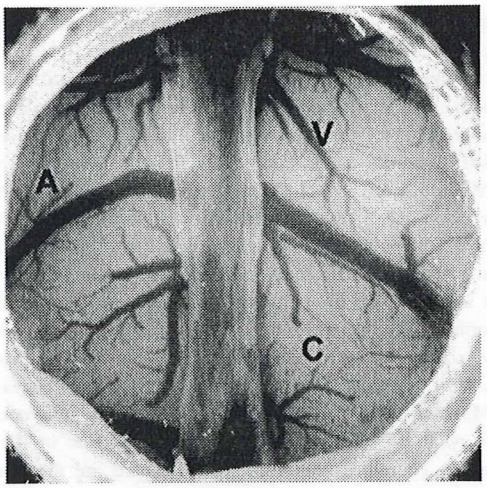

Fig. 1 Overview of the closed cranial window. The image was obtained using a light microscope. Three types of microvessels, arterioles (*A*), venules (*V*), and capillaries (*C*), were clearly observed in the rat pia mater 1 week after the window implantation

Table 1 The value of average SAR in the present experiment

Brain (W/kg)	0.6	2.4	4.8
Whole body (W/kg)	0.16	0.64	1.28

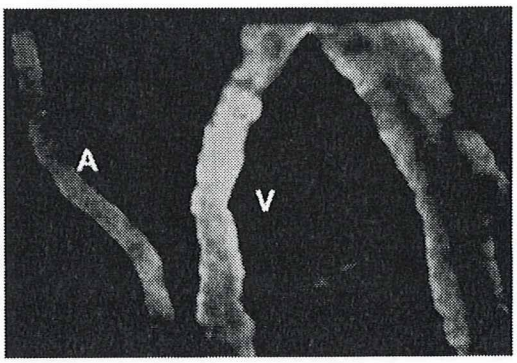

Fig. 2 Pial vessels observed by fluorescence microscopy. To evaluate the leakage level of fluorescent dye in detail, the fluorescent images of pial venule were observed using a confocal laser-scanning microscopic system. The fluorescence intensity of the image including arterioles (*A*), venules (*V*), and its surrounding extravascular region was measured at 5 s after the dye injection. No extravasation of the dye was observed in any area even after the subchronic exposure to RF-EMF for 4 weeks

TDMA (time division multiple access) signal for exposure was controlled by averaged SAR of the brain (Masuda et al. 2007b). The values of the averaged SAR were 0.6, 2.4, and 4.8 W/kg for acute exposure experiment and 2.4 W/kg for subchronic exposure experiment (Table 1). The exposure duration was 10 min for the acute exposure and was 60 min everyday, 5 days a week for 4 weeks, for subchronic exposure. In the subchronic experiments, the rats were randomly divided into three groups: exposed group (with RF-EMF), sham-exposed group (without RF-EMF), and cage-control group (just breeding in cages), consisting of ten rats each.

The pial microcirculatory parameters including vascular diameter, plasma velocity, leukocyte behavior, and BBB function within the cranial window were observed using intravital fluorescence microscopy (Fig. 2). The statistical analysis was carried out using a Mann–Whitney *U*-test or Kruskal–Wallis test followed by Scheffe test, and $P < 0.05$ values were considered statistically significant.

3 Results

In order to investigate the detail of hemodynamic changes and leukocyte behavior in the pial venule, each parameter

was separately measured at postcapillary venule (8–30 μm) and collecting venule (31–50 μm).

3.1 Effects of acute exposure

3.1.1 Permeability of blood-brain barrier

The changes in permeability of BBB after the exposure were evaluated using two molecules, sodium fluorescein (MW: 376) and FITC-dextran (MW: 250kDa), injected intravenously. Extravasation of sodium fluorescein from the pial venule was measured with the confocal scanning laser microscopy. In any measurement points, the fluorescence intensity profile in the inside and outside of the pial venule did not change at any SAR values. FITC-dextran was administered before RF-EMF exposure to detect the extravasation of dye during the exposure. The fluorescence intensity in the brain surface within pial microcirculation was measured until the end of experiment. However, there was no significant difference between sham group and exposed group in the time course of fluorescent intensity at any SAR values.

3.1.2 Hemodynamic changes

Plasma velocities and vessel diameters were measured for evaluation of the changes in hemodynamics after the exposure. Although the plasma velocity in postcapillary venule tended to increase at 2.4 and 4.8 W/kg, there were no significant differences in the velocities compared with pre-measurement or 0.6 W/kg of brain average SAR values. In collecting venule, no significant differences in the velocities were found among different exposures. The changes in diameter of pial venule were shown as a percentage of the pre-exposure diameter. There were no significant differences in the diameter.

3.1.3 Leukocyte behavior

The changes in leukocyte behavior were evaluated using the number of leukocytes having interactions with the endothelium of pial venule. Two states of interactions were identified: rolling and sticking. The rolling leukocytes were defined as cells having weak interactions with the endothelium, and thereby capable of rolling. The sticking leukocytes were defined as cells attached to the same endothelial area for more than 30 s. In postcapillary and collecting venules, the number of sticking leukocyte showed no significant difference between before and after the exposures. Although the number of rolling leukocyte tended to decrease corresponding to the increase in SAR values, there was no significant difference between before and after the exposure.

3.2 Effects of subchronic exposure

3.2.1 Permeability of blood-brain barrier

No leakage sites of sodium fluorescein in the pia mater were observed in any groups at 2 or 4 weeks after the beginning of the experiment. Although the fluorescence intensities in the pia mater region decreased time dependently after the intravenous injection of FITC-dextran, the intensities at each measurement period showed no significant differences between the three groups even after the exposure for 4 weeks.

3.2.2 Hemodynamic changes

Plasma velocities were measured for evaluation of the changes in hemodynamics after the exposure. There were no significant differences in the velocities among the three groups in both types of venules at any observation periods.

3.2.3 Leukocyte behavior

No effects of the RF-EMF exposure on the number of rolling leukocytes were observed in postcapillary venules or collecting venules. For the number of sticking leukocytes, no significant differences in the number between the three groups were found in either types of venule at any observation periods.

4 Discussion

We focused on the cerebral microcirculatory parameters and investigated the acute and subchronic effects on the exposure to RF-EMF on those parameters. As results of our studies, no significant changes were found at least in vascular diameters, plasma velocities, leukocyte behavior, or BBB function either after acute or subchronic exposure (Masuda et al. 2007). Although many investigators have reported the effects of RF-EMF on BBB permeability, these studies mainly used histological evaluation (Salford et al. 1994; Tsurita et al. 2000; Finnie et al. 2006; Fritze et al. 1997). On the contrary, we examined not only BBB permeability but also other microcirculatory parameters in vivo. Several reports have shown that the BBB disruption is accompanied with changes in leukocyte behaviors (Mayhan 2000; Gaber et al. 2004) or hemodynamics (Mayhan 1998) under inflammatory condition in the rat brain. Therefore, our findings obtained in the multi-parameters strengthen the negative results that the RF-EMF exposure does not induce BBB disruption.

In conclusion, the findings described in our recent reports suggested no noticeable changes in the BBB

function, the venular diameter, or the number of sticking leukocyte under the exposure conditions of RF-EMF that we used. However, further studies are required under other exposure conditions to confirm these phenomena.

Acknowledgments This work was financially supported by the committee to promote research on the possible biological effects of electromagnetic fields of the ministry of internal affairs and communications, Japan.

References

Finnie JW, Blumbergs PC, Cai Z, Manavis J, Kuchel TR (2006) Effect of mobile telephony on blood-brain barrier permeability in the fetal mouse brain. Pathology 38:63–65. doi:10.1080/00313020500459607

Fritze K, Sommer C, Schmitz B, Mies G, Hossmann KA, Kiessling M, Wiessner C (1997) Effect of global system for mobile communication (GSM) microwave exposure on blood-brain barrier permeability in rat. Acta Neuropathol 94:465–470. doi:10.1007/s004010050734

Gaber MW, Yuan H, Killmar JT, Naimark MD, Kiani MF, Merchant TE (2004) An intravital microscopy study of radiation-induced changes in permeability and leukocyte-endothelial cell interactions in the microvessels of the rat pia mater and cremaster muscle. Brain Res Brain Res Protoc 13:1–10. doi:10.1016/j.brainresprot.2003.11.005

Masuda H, Ushiyama A, Okano H, Ohkubo C (2000) 'Chronological observation of the pial microcirculation using a chronically implanted cranial window method in the rat'. In: Tsuchiya M, Asano M, Tokita T, Takahashi K (eds) Microcirculation Annual 2000. Nihon-Igakukan, Japan, pp 151–152

Masuda H, Ushiyama A, Hirota S, Lawlor GF, Ohkubo C (2007a) Long-term observation of pial microcirculatory parameters using an implanted cranial window method in the rat. In Vivo 21:471–479

Masuda H, Ushiyama A, Hirota S, Wake K, Watanabe S, Yamanaka Y, Taki M, Ohkubo C (2007b) Effects of acute exposure to 1439 MHz electromagnetic field on the microcirculatory parameters in rat brain. In Vivo 21:555–562

Masuda H, Ushiyama A, Hirota S, Wake K, Watanabe S, Yamanaka Y, Taki M, Ohkubo C (2007c) Effects of acute exposure to 1439 MHz electromagnetic field on the microcirculatory parameters in rat brain. In Vivo 21:563–570

Mayhan WG (1998) Effect of lipopolysaccharide on the permeability and reactivity of the cerebral microcirculation: role of inducible nitric oxide synthase. Brain Res 792:353–357. doi:10.1016/S0006-8993(98)00259-5

Mayhan WG (2000) Leukocyte adherence contributes to disruption of the blood-brain barrier during activation of mast cells. Brain Res 869:112–120. doi:10.1016/S0006-8993(00)02376-3

Mayhan WG (2001) Regulation of blood-brain barrier permeability. Microcirculation 8:89–104. doi:10.1038/sj.mn.7300154

Salford LG, Brun A, Sturesson K, Eberhardt JL, Persson BR (1994) Permeability of the blood-brain barrier induced by 915 MHz electromagnetic radiation, continuous wave and modulated at 8, 16, 50, and 200 Hz. Microsc Res Tech 27:535–542. doi:10.1002/jemt.1070270608

Tsurita G, Nagawa H, Ueno S, Watanabe S, Taki M (2000) Biological and morphological effects on the brain after exposure of rats to a 1439 MHz TDMA field. Bioelectromagnetics 21:364–371. doi:10.1002/1521-186X(200007)21:5<364::AID-BEM5>3.0.CO;2-Q

Yuan H, Gaber MW, McColgan T, Naimark MD, Kiani MF, Merchant TE (2003) 'Radiation-induced permeability and leukocyte adhesion in the rat blood-brain barrier: modulation with anti-ICAM-1 antibodies'. Brain Res 969:59–69. doi:10.1016/S0006-8993(03)02278-9

INTERNAL MEDICINE

□ ORIGINAL ARTICLE □

Relationships between Quantitative Electroencephalographic Alterations and the Severity of Hepatitis C Based on Liver Biopsy in Interferon-α Treated Patients

Satoshi Kamei[1], Akihiko Morita[1], Naohide Tanaka[2], Masato Matsuura[3], Mitsuhiko Moriyama[2], Takuya Kojima[3], Yasuyuki Arakawa[3], Yoshihiro Matsukawa[4], Tomohiko Mizutani[3], Teiichiro Sakai[3], Kentaro Oga[5], Hitoshi Ohkubo[6], Hiroshi Matsumura[7] and Kaname Hirayanagi[8]

Abstract

Objective We have observed alterations of quantitative (q)-EEG findings occurring in interferon (IFN)-α treated chronic hepatitis C (CH-C) patients, and found patient's age to be one factor influencing such EEG alterations. In the present study we evaluated the correlation between q-EEG alterations during IFN-α treatment and the severity of hepatitis based on liver biopsies.

Methods A total of 102 CH-C patients underwent blind, prospective and serial q-EEG examinations. The IFN-α was administered under the same therapeutic regimen to all patients. Serial EEGs were obtained before, at 2 and 4 weeks, and at 2-3 days after the conclusion of treatment. The absolute powers of each frequency band in different periods were determined by q-EEG. Staging (of fibrosis) and grading (of inflammatory cell infiltration) were scaled according to Desmet's classification. We evaluated the relationship between q-EEG and scales of staging or grading.

Results Age distributions did not differ significantly among stages or grades. As the stage or grade increased, the alterations of EEG during IFN-α treatment became more pronounced, and significant (repeated-measures analysis of variances; both, $p<0.0001$).

Conclusion Alterations of the EEG occurring during IFN-α treatment became pronounced with more severe pathological findings for CH-C. Alterations in the EEGs during IFN-α treatment should be carefully monitored in CH-C patients with severe pathological findings.

Key words: interferon-α, quantitative-EEG, chronic hepatitis C, staging, grading

(Inter Med 48: 975-980, 2009)
(DOI: 10.2169/internalmedicine.48.1902)

Introduction

Alterations of brain waves on electroencephalograms (EEGs) during treatment with interferon (IFN)-α have been described previously in several case reports (1-3). We have confirmed a diffuse slowing based on an analysis of blind, prospective and serial quantitative-EEG (q-EEG) examina-

[1]Division of Neurology, Department of Medicine, Nihon University Itabashi Hospital, Tokyo, [2]Division of Gastroenterology and Hepatology, Department of Medicine, Nihon University Itabashi Hospital, Tokyo, [3]Department of Neuropsychiatry, Nihon University Itabashi Hospital, Tokyo, [4]Division of Hematology and Rheumatology, Department of Medicine, Nihon University Itabashi Hospital, Tokyo, [5]Department of Neuropsychiatry, Nihon University Surugadai Hospital, Tokyo, [6]Department of Internal Medicine, Nihon University Surugadai Hospital, Tokyo, [7]Department of Internal Medicine, Itabashi Medical Association Hospital, Tokyo and [8]Department of Hygiene and Public Health, Nihon University of Physical Education, Tokyo

Received for publication November 28, 2008; Accepted for publication March 11, 2009

Correspondence to Dr. Satoshi Kamei, skamei@med.nihon-u.ac.jp

Table 1. Mean Values and Standard Deviations of Age for Each Stage and Grade Based on Liver Biopsies in 102 Subjects

Findings of liver biopsy	Number of patients	Mean ± standard deviation of patients' age (years old)	Difference in mean values between different stages or grades (Mann-Whitney U test)
Stage (intrahepatic fibrosis)			
Mild	49	48.4 ± 6.1	
Moderate	38	51.9 ± 7.4	NS
Severe	15	46.9 ± 8.9	
Grade (inflammatory cell infiltration)			
Minimal	43	48.2 ± 6.0	
Mild	30	50.6 ± 7.1	NS
Moderate	14	51.3 ± 6.6	
Severe	15	47.3 ± 8.8	

NS = not significant.

tions undertaken in many patients with IFN-α treated chronic hepatitis C (4). We speculated that such diffuse slowing on the EEGs could reflect a mild encephalopathy due to the IFN-α. We recently reported that the alteration of the q-EEG could be estimated clinically by the change in score on Mini-Mental State Examinations (5). We have also reported that the age of the patients was one of the factors affecting such alterations on the q-EEG (6). However, no other such factors have been reported. The present study was the first to evaluate the relationship between the alterations in q-EEG findings that occur during IFN-α treatment and the severity of hepatitis as estimated according to scales of staging and grading based on liver biopsies.

Methods

Patients

A total of 168 serial patients with chronic hepatitis C patients underwent our blind, prospective and serial q-EEG examinations, during the period from August 1997 to May 2007. These patients were independently registered at three different hospitals, viz. Nihon University Itabashi Hospital, Nihon University Surugadai Hospital, and Itabashi Medical Association Hospital, during the above period. All patients were investigated and treated under the same clinical regimen and conditions, including diagnostic criteria, q-EEG examinations, and IFN-α treatment, as reported previously (4). The clinical diagnosis of chronic hepatitis C was confirmed by serological findings of serum antibody for hepatitis C virus, histopathological findings obtained by liver biopsy, detection of the viral genome sequence for hepatitis C virus by the reverse transcriptase-polymerase chain reaction (RT-PCR), serum liver function tests, and the clinical course of the patients. Staging (of intrahepatic fibrosis) and grading (of inflammatory cell infiltration) of the chronic hepatitis based on liver biopsies was scored according to Desmet's classification (7). Based on grading of histopathological findings according to the Desmet's classification (7), the patients with liver cirrhosis (LC) were excluded from the present study. A total of 102 patients ranging in age from 40 to 59 years were included in this study. All patients were alert during IFN-α treatment as graded according to the Glasgow Coma Scale. The mean values and standard deviations of patient age at each stage and grade of chronic hepatitis are listed in Table 1. There were no significant differences in mean age among stages or grades (Mann-Whitney U test). IFN-α was administered intramuscularly at a dose of 9×10^6 IU daily for the first 4 weeks and then administered 3 times/week for the following 20 weeks, according to the same regimen of IFN-α treatment. Informed consent to perform the present study was obtained from all patients. The serological hepatic function parameters of the 102 patients improved during the IFN-α treatment. The means and standard deviations for the values of AST (GOT) (normal: 8-38 IU/L) were 126.2±75.1 before the treatment, 50.7±23.6 at 2 weeks of treatment, 43.2±24.1 at 4 weeks of treatment, and 40.4±23.1 IU/L after the treatment. The values for ALT (GPT) (normal: 4-44 IU/L) were 164.1±93.2 before the treatment, 60.4±33.2 at 2 weeks of treatment, 55.0±29.1 at 4 weeks of treatment, and 52.4±27.1 IU/L after the treatment. No patients exhibited elevation of serological hepatic function parameters during IFN-α treatment. There were also no patients with significant elevation of serum ammonia concentration during this treatment. All of the patients gave informed consent to participate in the present study according to a protocol approved by the Ethics Committee for Human Studies at Nihon University.

Q-EEG analysis

The EEG recordings and q-EEG analysis employed in the present study were as described previously (4). Briefly, serial EEGs were obtained before the IFN treatment, at 2 and 4 weeks of treatment and at 2-3 days after the conclusion of treatment. The serial EEGs at 2 and 4 weeks of treatment were obtained during the period from 1 to 6 hours after the injection of IFN-α. The EEGs in each subject were recorded on a magnetic optical disk from 16 electrode locations according to the 10-20 international system using a digital EEG instrument (Neurofax EEG-4518, Nihon Kohden, To-

kyo, Japan). The EEGs were referenced to the ipsilateral earlobes. Sixty seconds of q-EEG data were selected visually from each subject and digitized at 128 Hz with a time constant of 0.3, employing a high frequency filter of 60 Hz. Thirty epochs with a duration of 2 seconds each were collected from the subsequent resting period with eyes closed for analysis of the q-EEGs. The procedure used for analysis involved the application of fast Fourier transformation of the collected EEG signals by Rhythm, version 10.0 (Stellate Systems Inc, Montreal, Quebec, Canada). The frequency ranges were divided into 6 bands, as follows: delta (1.17-3.91 Hz), theta 1 (4.30-5.86 Hz), theta 2 (6.25-7.81 Hz), alpha 1 (8.20-10.16 Hz), alpha 2 (10.55-12.89 Hz), and beta (13.28-30.86 Hz). The absolute powers of each frequency band were calculated at each electrode location in all of the subjects. Each power value was obtained by integrating the appropriate part of the spectrum. The present quantitative analysis was carried out blindly during routine EEG work involving many other disease states, including epilepsy, cerebrovascular disease, encephalitis, meningitis, metabolic encephalopathy, and brain tumor, as well as in normal controls. The only knowledge that the EEG analyst (S. Kanei) possessed regarding each patient was the latter's identification number, and he had no other information regarding any other information concerning any of the studied subjects such as their clinical diagnosis, date of treatment, or type of treatment.

Statistical analysis

In September 2007, a statistical analyst (K. Hirayanagi) at another independent institute collected the analyzed q-EEG data, the data on patient ages, and that on histopathological findings on liver biopsy based on the Desmet's classification (7) for the 102 patients. Using Desmet's classification (7), the stage of intrahepatic fibrosis in each sample was classified as mild, moderate, or severe. The grade of inflammatory cell infiltration in each sample was classified as follows: minimal, mild, moderate, or severe. The distributions of the power values at each frequency band for each electrode location were evaluated in terms of their skewness and kurtosis. Based on findings regarding skewness and kurtosis, repeated measure analysis of variances (rANOVAs) was applied to the alterations in power values as the main factor among 4 different periods: before the IFN-α treatment, at 2 and 4 weeks of treatment, and after the treatment, with the frequency bands, electrode locations, and staging and grading on the hepatitis classifications as co-factors. SPSS statistical software Version 12.0 (SPSS Inc., Chicago, IL) was employed for statistical analysis. Relationships between q-EEG variables and stages or grades were evaluated by post hoc ANOVAs (Scheffe's test). The level of significance for this study was 0.05.

Results

There were no patients with IFN-α induced irreversible encephalopathy in the present study. Stages of the chronic hepatitis based on liver biopsies in the 102 subjects were distributed over the range from mild to severe fibrosis. Similarly, grades were also distributed from minimal to severe inflammatory cell infiltration. The results of serial q-EEG studies at each selected frequency of EEG during the IFN-α treatment for each staging and grading scale (Figs. 1, 2) revealed that increased slow waves (delta, theta 1 and 2) and decreased alpha 2 and beta waves were evident during the IFN-α treatment at all stages and grades. These EEG alterations during IFN-α treatment in the present study confirmed our previously reported observations (4). Moreover, the alterations in power values during the IFN-α treatment became more pronounced as the stage or grade of hepatitis increased. Statistical results obtained by rANOVAs (Table 2) for the interactions between the q-EEG alterations during the IFN-α treatment and differences of staging scale or grading scale were significant (both, $p<0.0001$). Results of post hoc ANOVAs results (Table 3) also indicated significant differences in the alterations of absolute power values during the IFN-α treatment for all comparisons with increasing staging or grading scale in the case of the delta, theta 1, and beta waves with the exception of several comparisons involving differences of only one grade or stage. There were no significant differences in the alterations of power values during the IFN-α treatment in the case of the alpha 1 and total power values. We also examined the correlations at each electrode location between severity based on liver biopsy findings and alteration of qEEG during the administration of IFN-α. These correlations were significant for all electrode locations (frontal pole location $p=0.03$ and $p=0.004$ for stage and grade, respectively; frontal location $p<0.0001$ for both stage and grade; temporal location $p<0.0001$ for both; central location $p=0.005$ and $p=0.002$; parietal location $p=0.002$ and $p=0.01$; occipital location $p=0.005$ and $p=0.01$).

There were only two patients with mild pyrexia (37.3 and 37.4℃) at the time of q-EEG examination after 2 weeks of IFN-α administration, and no patient with pyrexia at the time of examination at 4 weeks. The two patients with mild pyrexia had findings of mild severity on liver biopsy. No significant effects of pyrexia on q-EEG were found.

Discussion

Although numerous patients have undergone IFN-α treatment, detailed assessments of the adverse effects of IFN-α on central nervous system function have not yet been presented. Evaluations of alterations in brain function have been presented in only three previous reports based on data from small numbers of patients who underwent EEG examinations (1-3). We recently confirmed a significant, diffuse slowing on q-EEGs that occurred in chronic hepatitis C patients during IFN-α treatment at a relatively low dosage (4). With such a low dosage of IFN-α administration to chronic hepatitis C patients, the diffuse slowing of the EEG is re-

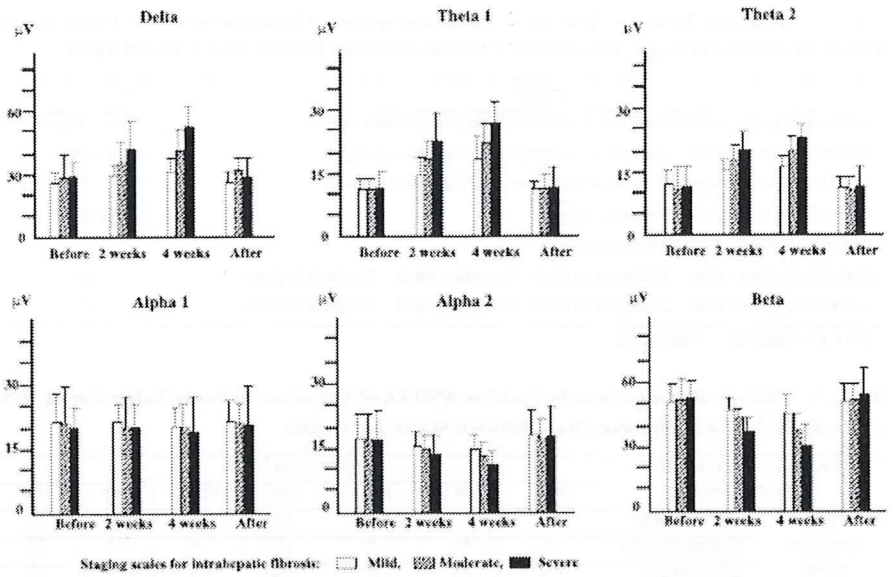

Figure 1. Alterations in absolute power values (means±standard deviations) by stage (of intrahepatic fibrosis) for each frequency band at the following 4 time points: before IFN-α treatment, at 2 and 4 weeks of treatment, and at 2-3 days after conclusion of treatment. Increasing power values for slow waves (delta, theta 1 and 2) and decreasing power values for alpha 2 and beta waves during IFN-α treatment, in comparison with those before and after IFN-α treatment, were evident for all stages. Moreover, alterations in power values became more pronounced as stage increased in all frequency bands except for alpha 1 and total power values.

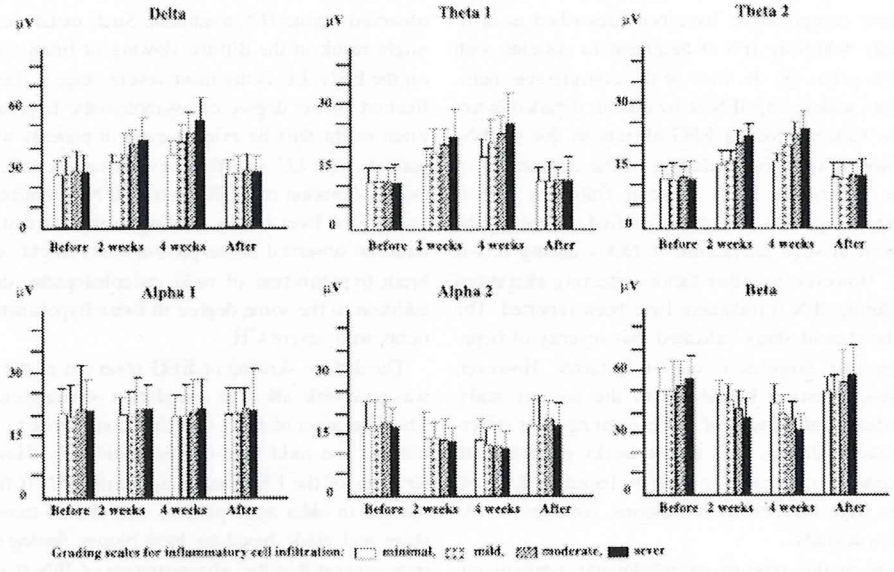

Figure 2. Alterations in absolute power values (means±standard deviations) by grade (of inflammatory cell infiltration) for each frequency band at the following 4 time points: before IFN-α treatment, at 2 and 4 weeks of treatment, and at 2-3 days after conclusion of treatment. Increasing power values for slow waves (delta, theta 1 and 2) and decreasing power values for alpha 2 and beta waves during IFN-α treatment, in comparison with those before and after IFN-α treatment, were evident for all grades. Moreover, the alterations in power values became more pronounced with increase in grade in all frequency bands except for alpha 1 and total power values.

Table 2. Repeated Measures Analysis of Variances between Alterations in Power Values during IFN-α Treatment and Stage (Intrahepatic Fibrosis) or Grade (Inflammatory Cell Infiltraion)

Factors	
Alteration of power values during IFN-α treatment (Alteration of power values)	p< 0.0001 (F=30.338)
Alteration of power values × Difference of staging scale (Difference in stage)	p< 0.0001 (F=14.531)
Alteration of power values × Difference of grading scale (Difference in grade)	p< 0.0001 (F=12.071)
Alteration of power values × Frequency bands	p< 0.0001 (F=48.781)
Alteration of power values × Electrode location	NS
Alteration of power values × Difference in stage × Frequency bands × Electrode location	NS
Alteration of power values × Difference in grade × Frequency bands × Electrode location	NS

NS = not significant; × = interaction.

Table 3. Statistical Comparisons by Post-hoc ANOVA of Alterations in Power Values during IFN-α Treatment for Each Frequency Band between Stages and Grades

Comparison of stages and grades based on biopsies		Power values (μV)						
		delta	theta 1	theta 2	alpha 1	alpha 2	beta	total
Stage (intrahepatic fibrosis)	mild vs. moderate	**	**	*	NS	NS	**	NS
	moderate vs. severe	**	**	**	NS	*	**	NS
	mild vs. severe	**	**	**	NS	*	**	NS
Grade (inflammatory cell infiltration)	minimal vs. mild	**	**	**	NS	NS	*	NS
	minimal vs. moderate	**	**	**	NS	*	**	NS
	minimal vs. severe	**	**	**	NS	*	**	NS
	mild vs. moderate	**	**	**	NS	NS	*	NS
	mild vs. severe	**	**	**	NS	*	**	NS
	moderate vs. severe	**	**	**	NS	*	**	NS

NS = not significant, * = $0.01 \le p < 0.05$, ** = $p < 0.01$.

versible after completion of the treatment (4). Moreover, neuropsychiatric complications have been described as difficult to evaluate following IFN-α treatment in patients with chronic viral hepatitis (8). In view of the considerable numbers of patients undergoing IFN-α treatment, detailed information on the factors affecting EEG alterations due to IFN-α treatment seems vital for prediction of the appearance of such adverse effects on brain function following IFN-α treatment. Patient age was recently identified as one of the factors involved in such alterations of EEGs during IFN-α treatment (6). However, no other factors affecting alterations of the EEG during IFN-α treatment have been reported. The findings of the present study indicated that severity of hepatitis based on liver biopsies is one such factor. However, there are some statistical limitations to the present study. Since we evaluated alterations of q-EEG during four different periods (pre-treatment, at 2 and 4 weeks of treatment, and post-treatment), the scales of severity based on liver biopsy findings were handled as continuous variables in rANOVA of present study.

The etiology of this type of encephalopathy remains unclear regarding whether it involves direct or indirect toxic effects on the central nervous system. Several possible indirect mechanisms can be considered. IFN plays a role in the production of secondary cytokines such as interleukin-1 and tumor necrosis factor (9). Neuroendocrine hormone alterations may also be induced by IFN. IFN displays structural and functional similarities to neuroendocrine hormones such as ACTH (10, 11), and increased cortisol levels have been observed during IFN treatment. Such metabolic vulnerability might result in the diffuse slowing of brain waves observed on the EEG. LC is the most severe stage in Desmet's classification. Some degree of asymptomatic hypofunction of the brain might thus be evident even in patients with CH, as in patients with LC. Our finding of a significant correlation between alteration of qEEG during IFN administration and the severity of liver biopsy findings suggests that the EEG alterations observed in the present study might be detected the brain hypofunction of mild encephalopathy due to IFN in addition to the some degree of brain hypofunction in the patients with severe CH.

The diffuse slowing of EEG observed in the present study was reversible after the completion of treatment (Figs. 1, 2). This alteration of EEG was thus considered to be an asymptomatic and mild type of encephalopathy. However, the alterations of the EEG occurring during IFN-α treatment were marked in older aged patients and also in those with a high stage and grade based on liver biopsy findings. These findings suggest that the administration of IFN-α should be discontinued in patients with neuropsychiatric complications such as depression in the presence of EEG slowing. Serial EEG monitoring thus appears to be of value in detecting alterations of brain function during IFN-α treatment in chronic viral hepatitis patients, and alterations on serial EEGs should be carefully monitored in older patients and in those with severe stage and grade on liver biopsies.

Acknowledgement

The present study was performed as one of the works of the Research Group for Comprehensive Clinical Studies on the Diagnosis, Treatment and Prevention of Neurological Disorders, which was supported by a Research Grant (18A-9) for Nervous and Mental Disorders from the Ministry of Health, Labour and Welfare, Japan, and a Grant from the Ministry of Science and Culture for the Promotion of Research Foundation.

References

1. Rohatiner AZS, Prior PF, Burton AC, Smith AT, Balkwill FR, Lister TA. Central nervous system toxicity of interferon. Br J Cancer **47**: 419-422, 1983.
2. Smedley H, Kartrak M, Sikora K, Wheeler T. Neurological effects of recombinant interferon. Br Med J **286**: 262-264, 1983.
3. Meyers CA, Scheibel RS, Forman AD. Persistent neurotoxicity of systemically administered interferon-alpha. Neurology **41**: 672-676, 1991.
4. Kamei S, Tanaka N, Matsuura M, et al. Blinded, prospective, and serial evaluation by quantitative-EEG in interferon-alpha-treated hepatitis-C. Acta Neurol Scand **100**: 25-33, 1999.
5. Kamei S, Sakai T, Matsuura M, et al. Alterations of quantitative EEG and Mini-Mental State Examination in interferon-α-treated hepatitis C. Eur Neurol **48**: 102-107, 2002.
6. Kamei S, Oga K, Matsuura M, et al. Correlation between quantitative-EEG alterations and age of IFN-α treated hepatitis C patients. J Clin Neurophysiol **22**: 49-52, 2005.
7. Desmet VJ, Gerber M, Hoofnagle JH, Manns M, Scheuer PJ. Classification of chronic hepatitis: diagnosis, grading and staging. Hepatology **19**: 1513-1520, 1994.
8. Saracco G, Rizzetto M. Therapy of Chronic Viral Hepatitis. In: Oxford Textbook of Clinical Hepatology. 1. 2nd ed. Bircher J, Benhamou J-P, McIntyre N, et al, Eds. Oxford University Press, Oxford, 1999; 939-954.
9. Arenzana-Seisdedos F, Virelizier JL. Interferons as macrophage-activating factors. II: enhanced secretion of interleukin-1 by lipopolysaccharide-stimulated human monocytes. Eur J Immunol **13**: 437-440, 1983.
10. Blalock JE, Smith EM. Human leukocyte interferon: structural and biological relatedness to adrenocorticotropic hormone and endorphins. Proc Natl Acad Sci USA **77**: 5972-5974, 1980.
11. Blalock JE, Stanton JD. Common pathway of interferon and hormonal action. Nature **283**: 406-408, 1980.

© 2009 The Japanese Society of Internal Medicine
http://www.naika.or.jp/imindex.html

Provided for non-commercial research and education use.
Not for reproduction, distribution or commercial use.

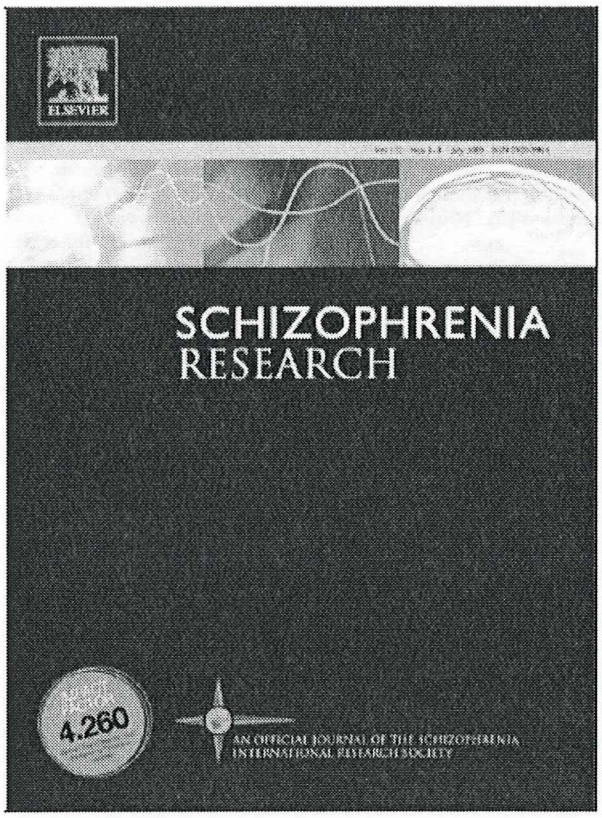

This article appeared in a journal published by Elsevier. The attached copy is furnished to the author for internal non-commercial research and education use, including for instruction at the authors institution and sharing with colleagues.

Other uses, including reproduction and distribution, or selling or licensing copies, or posting to personal, institutional or third party websites are prohibited.

In most cases authors are permitted to post their version of the article (e.g. in Word or Tex form) to their personal website or institutional repository. Authors requiring further information regarding Elsevier's archiving and manuscript policies are encouraged to visit:

http://www.elsevier.com/copyright

Schizophrenia Research 112 (2009) 149–152

Contents lists available at ScienceDirect

Schizophrenia Research

journal homepage: www.elsevier.com/locate/schres

Impact of changing the Japanese term for "schizophrenia" for reasons of stereotypical beliefs of schizophrenia in Japanese youth

Hidehiko Takahashi [a,b,*], Takashi Ideno [c], Shigetaka Okubo [c], Hiroshi Matsui [d], Kazuhisa Takemura [c], Masato Matsuura [b], Motoichiro Kato [e], Yoshiro Okubo [f]

[a] Department of Molecular Neuroimaging, National Institute of Radiological Sciences, 4-9-1, Anagawa, Inage-ku, Chiba, 263-8555, Japan
[b] Department of Life Sciences and Bio-Informatics, Graduate School of Health Sciences, Tokyo Medical and Dental University, 1-5-45 Yushima, Bunkyo-ku, Tokyo, 113-8519, Japan
[c] Department of Psychology, Waseda University, 1-24-1 Toyama, Shinjyuku-ku, Tokyo, 162-8644, Japan
[d] Department of Sociology, Rikkyo University, Nishikebukuro, Toshima-ku, Tokyo, 171-8501, Japan
[e] Department of Neuropsychiatry, Keio University School of Medicine, 35 Shinanomachi, Shinjyuku-ku, Tokyo, 160-8582, Japan
[f] Department of Neuropsychiatry, Nippon Medical School, 1-1-5 Sendagi, Bunkyo-ku, Tokyo, 113-8602, Japan

ARTICLE INFO

Article history:
Received 9 July 2008
Received in revised form 30 March 2009
Accepted 31 March 2009
Available online 23 April 2009

Keywords:
Schizophrenia
Stigma
Implicit association test
Renaming

ABSTRACT

The old term for schizophrenia, "Seishin-Bunretsu-Byo" (Mind-Split Disease), has been replaced by "Togo-Shitcho-Sho" (Integration Disorder) in Japan. Stigma research requiring individuals to report personal beliefs is useful but is subject to social desirability bias. Using the Implicit Association Test, a measurement designed to minimize this bias, we assessed the impact of this renaming on the stereotype of schizophrenia held by a younger generation. The old term was strongly associated with "criminal", and this association became significantly weaker with the new term. The strategy of renaming holds considerable promise for tempering negative bias toward this disorder in Japan.

© 2009 Elsevier B.V. All rights reserved.

1. Introduction

The stigma of mental disorders stands in the way of improving the quality of life of people with disorders as well as their families. The stigma leads to discriminations in education, employment, personal relationships, marriage and housing. To reduce mental illness-related stigma (particularly regarding schizophrenia), various programs are underway internationally (Sartorius, 2007; Thornicroft et al., 2007). In Japan as well, a strategy to change the term for schizophrenia was introduced. Since each Chinese character conveys its own meaning, and the old term for schizophrenia, "Seishin-Bunretsu-Byo", explicitly translates as "Mind-Split-Disease", the Japanese Society of Psychiatry and Neurology approved replacing the old term with "Togo-Shitcho-Sho", literally meaning "Integration Disorder". The former term has been said to lead the public to misunderstand and stigmatize individuals with schizophrenia.

In western society, the term also implies "split" and is frequently misunderstood as "split personality" (Chopra and Doody, 2007) or inappropriately metaphorized (Geller, 2001). In fact, even in a renowned scientific journal, "schizophrenia" was recently misused as "split personality" (May, 2008; Pfleiderer and Hackl, 2007). Thus, movements to rename schizophrenia are gaining momentum in western society as well (Kingdon et al., 2007). Most stigma research relies on questionnaires that require individuals to report their personal attitude (Greenwald and Banaji, 1995; Hinshaw and Stier, 2008). This information is useful but is subject to response bias due to social desirability (Dovidio et al., 1997;

* Corresponding author. Department of Molecular Neuroimaging, National Institute of Radiological Sciences, 4-9-1, Anagawa, Inage-ku, Chiba, 263-8555, Japan. Tel.: +81 43 206 3251; fax: +81 43 253 0396.
E-mail addresses: hidehiko@nirs.go.jp (H. Takahashi), idenodei@gmail.com (T. Ideno), anything_goes@akane.waseda.jp (S. Okubo), matsui.hiroshi@gmail.com (H. Matsui), kazupsy@waseda.jp (K. Takemura), matsu.mtec@tmd.ac.jp (M. Matsuura), katomoto@sc.itc.keio.ac.jp (M. Kato), okubo-y@nms.ac.jp (Y. Okubo).

0920-9964/$ – see front matter © 2009 Elsevier B.V. All rights reserved.
doi:10.1016/j.schres.2009.03.037

Gaebel et al., 2002; Griffiths et al., 2006; Hinshaw and Stier, 2008). One measure designed to minimize response bias is the Implicit Association Test (IAT) (Greenwald et al., 1998). IAT assesses associations that exist beyond conscious evaluation, allowing a measurement of automatic biases even if people are unaware or unwilling to report them. This method has been widely used to assess implicit attitudes and stereotypes associated with many characteristics, including age, race and gender (Greenwald et al., 2002). Recently, IAT has been applied to the assessment of negative attitude toward mental illness (Teachman et al., 2006). Using IAT, we assessed the impact of renaming on the implicit stigma associated with this disorder in Japan. The most prevalently held stereotype is that of people with mental illness being unpredictable and dangerous (Angermeyer and Matschinger, 2004). The media are an important source of public information on mental illness (Stark et al., 2004), and negative depictions (criminality and dangerousness) of mental illness predominate (Coverdale et al., 2002). The media tend to present sensationalized and stereotypic depictions of mental illness and emphasize propensities toward violence and crime (Hinshaw and Stier, 2008). However, previous studies have revealed that people with mental illness are far more likely to be victims of crime than perpetrators (Hinshaw and Stier, 2008; Teplin et al., 2005). We assessed the association between schizophrenia and criminal versus victim. We hypothesized that the new term would have less automatic association with criminal.

2. Materials and methods

2.1. Participants

Sixty-eight non-medical undergraduate students (28 males and 40 females, mean age 21.5 years, S.D. = 1.4) participated. All were Japanese. They were asked if they were aware of the replacement of the term for schizophrenia. They were further asked about their knowledge of schizophrenia using a 7-point scale (1= none, 7= very much). The average score of knowledge was 3.5, indicating that the participants did not have enough or accurate knowledge of schizophrenia, although the majority (88%) knew of the renaming from the media. After complete explanation of the study, written informed consent was obtained from all participants, and the study was approved by the Ethics Committee.

2.2. Measures and procedures

To assess explicit attitudes, participants reported their attitude about mental illness using the Japanese version of the 4-point Link's devaluation–discrimination scale (Link, 1987; Shimotsu et al., 2006), a 12-item scale that has been widely used to measure stigma in relation to mental illness. Each item is designed to report what a subject thinks most people's opinion is concerning mental illness rather than to report the subject's own opinion. The items include, for example, "Most people think less of a person who has been in a mental hospital." Each statement is rated on a 4-point scale ranging from "strongly disagree = 1" to "strongly agree = 4", yielding a total score from 12 to 48.

To assess the automatic association between schizophrenia and criminal, IAT was administered according to standard procedures (Greenwald et al., 1998). Briefly, a physical chronic illness, diabetes mellitus, was used for comparison, since schizophrenia is a generally chronic illness, and awareness of comorbid diabetes in schizophrenia has been increasing with the introduction of atypical antipsychotics. The associations of these illnesses with two attributes (criminal and victim) were assessed. We conducted an initial survey to select target words associated with schizophrenia, diabetes, criminal and victim. Twenty university students other than the participants of this study were screened. They were asked to come up with up to 30 words associated with each of schizophrenia, diabetes, criminal and victim. We selected the most commonly proposed 10 words for each. Then an experienced psychologist (TI), who was a trained experimenter of IAT, and two experienced psychiatrists (HT and MK) assessed the selected words in terms of word length, complexity, familiarity and clarity. Five words for each category meeting a consensus were finally selected. Schizophrenia (hallucination, delusion, psychiatry, bizarre, seclusion), diabetes (obesity, insulin, diet, sugar, internal medicine), criminal (violence, jail, murder, theft, robbery) and victim (disaster, family, accident, casualty, the bereaved) stimuli appeared in the center of the computer screen. In congruent condition (CC), the concept "schizophrenia" and attribute "criminal" were paired in the top left corner while "diabetes" and "victim" were simultaneously paired in the top right corner. Participants were told to classify any stimuli that belonged to either the schizophrenia or criminal categories on the left, and any that belonged to either the diabetes or victim categories on the right, as quickly as possible by pressing a left or right button. In incongruent condition (IC), the labels were switched and the same categorization task was completed while pairing "schizophrenia" with "victim" and "diabetes" with "criminal". There were 40 trials for both CC and IC. Since negative attitudes toward mental illness are observed in many cultures (Kadri and Sartorius, 2005), it was predicted that CC categorizations would be easier and thus made more quickly than IC ones. Strong implicit associations should lead to fast congruent and slow incongruent categorizations. As a result, the IAT effect (reaction time for IC minus CC) provides a measure of the strength of implicit associations. To examine the impact of changing the term for schizophrenia, 2 versions of IAT were run for each participant. The old term for schizophrenia was used in one version, and the new term in the other version. The order of the two versions was counterbalanced across the subjects.

3. Results

The average total score of Link's devaluation–discrimination scale was 31.9 (S.D. = 5.5). This was in very good agreement with the study of reliability and validity of the Japanese translated version, in which the average total scores for males and females were 31.6 and 31.9, respectively (Shimotsu et al., 2006).

For the "Seishin-Bunretsu-Byo" version, average response latency for CC and IC was 844 ms (SEM = 21) and 927 ms (SEM = 25), respectively, yielding an 84-ms averaged IAT effect. For the "Togo-Shitcho-Sho" version, average response latency for CC and IC was 871 ms (SEM = 24) and 892 ms (SEM = 23), respectively, yielding a 21-ms averaged IAT effect.